A Phase Field Model Incorporating Generic and Specific Prior Knowledge Applied to Road Network Extraction from VHR Satellite Images

Ting Peng[1,2], Ian H. Jermyn[1], Véronique Prinet[2], Josiane Zerubia[1], BaoGang Hu[2]
[1]Ariana (joint research group INRIA/I3S), INRIA, B.P. 93,
06902 Sophia Antipolis, France. Email: firstname.lastname@sophia.inria.fr
[2]LIAMA, Institute of Automation, Chinese Academy of Sciences,
Beijing 100080, China. Email: prinet@nlpr.ia.ac.cn

Abstract

We address the problem of updating road maps in dense urban areas by extracting the main road network from a very high resolution (VHR) satellite image. Our model of the region occupied by the road network in the image is innovative. It incorporates three different types of prior geometric knowledge: generic boundary smoothness constraints, equivalent to a standard active contour prior; knowledge of the geometric properties of road networks (*i.e.* that they occupy regions composed of long, low-curvature segments joined at junctions), equivalent to a higher-order active contour prior; and knowledge of the road network at an earlier date derived from GIS data, similar to other 'shape priors' in the literature. In addition, we represent the road network region as a 'phase field', which offers a number of important advantages over other region modelling frameworks. All three types of prior knowledge prove important for overcoming the complexity of geometric 'noise' in VHR images. Promising results and a comparison with several other techniques demonstrate the effectiveness of our approach.

1 Introduction

Keeping the information contained in Geographical Information Systems (GIS) up to date is crucial for many applications, for example urban planning, vehicle navigation, and environmental monitoring. The high rate of urban growth, especially in many developing countries, means that this has become an increasingly important research topic in remote sensing. Very high resolution (VHR) optical satellite images (*e.g.* QuickBird and Ikonos, and Pléiades in the near future), with sub-metric resolutions, already facilitate the updating process due to their relatively low cost, high acquisition frequency, and rich information content, but current methods, based on manual extraction, are time and labour intensive, and often surprisingly inaccurate. The development of automatic GIS updating systems is thus a necessity if the increasing demand is to be met.

In this paper, we address the updating problem for road networks, and in particular the problem of automatically updating the GIS map of main roads in Beijing using a single QuickBird panchromatic image with 0.6m resolution. Unfortunately, even restricting to

the case of road networks, the automatic updating problem is not easily solved. To extract the road network from VHR images—formally, to find the region R in the image domain Ω that contains the roads—means to ignore the wealth of 'noise' that such images contain, for instance shadows, occlusions, and entities that locally appear similar to roads. This 'noise' means that the road network cannot be identified using only the information contained in the data; a great deal of prior knowledge, in this case concerning R, must also be injected. This is particularly true in an urban environment, where the degree of 'clutter' in the image is far greater than in the peri-urban or rural cases. This prior knowledge is currently provided by the human operators who manually extract the information; the question is how to incorporate a similar quantity of prior knowledge automatically.

The knowledge needed lies at different levels of generality. The most general concerns the regularity properties of the boundary ∂R of R. These properties apply to almost any entity, not only road networks. As a consequence, this prior knowledge is included in almost all region models, *e.g.* the Ising model, and most active contour models [7]. It suffices to include a term penalizing the length of ∂R. The most specific concerns the particular road network under consideration. Seen in a more general context as 'shape modelling', this has been the subject of a number of papers in recent years, *e.g.* [3, 4, 8, 9, 14]. This type of knowledge says that the region sought must be 'close' to an exemplar region. When such an exemplar exists, *e.g.* a GIS map of the road network at an earlier date, it can significantly increase the robustness of the method. For example, Bailloeul [2] makes use of cartographic data by constraining an active contour to resemble the shape template provided by vectorized GIS building maps. Fortier et al. [5] initialize the contour using a GIS map and junctions detected in the image. The contour then corrects the position of the existing road network. Agouris et al. [1] compute a positional uncertainty for each contour point in a GIS map using fuzzy logic. An energy term measuring shape uncertainty is then used to control an active contour.

Between these two extremes is prior geometric knowledge that applies to any road network. In some ways, this is the most difficult type of prior knowledge to include in a model, mainly because the regions corresponding to road networks can possess arbitrary topology: there may be many connected components, and each connected component may contain many loops. It is a non-trivial task to combine this topological freedom with the available geometric information: road network regions are composed of long, low curvature segments of roughly constant width that join at junctions. For example, Péteri and Ranchin [11] address the problem of extracting the road network from an Ikonos satellite image in a dense urban area. They introduce geometric knowledge via a parallelism constraint on the contours representing the borders of the roads, but they avoid the topology problem by assuming that a graph of the network is given. Roads and junctions are then extracted in two steps using two different types of active contours. Rochery et al. [13] on the other hand, address the problem of road network extraction from low to medium resolution images using a modelling framework known as 'higher-order active contours'. This framework allows the inclusion of prior geometric information without necessarily constraining the topology because, rather than relying on an exemplar region, it uses long-range interactions between contour points to control region geometry. Rochery et al. [12] address road network extraction using a reformulation of HOACs as (nonlocal) phase field models. The phase field approach to region modelling, which we also use in this paper, has a number of advantages, even for the simplest models, but in particular for HOACs. Peng et al. [10] apply the work of Rochery et al. [12] to VHR images using a multiscale

data energy to deal with the complexity of such images.

In this paper, we make two main contributions with respect to this literature. In problem-specific terms, we make progress towards an automatic road map updating system for VHR images. In methodological terms, we construct a model that combines the three types of prior knowledge described above, and express them all as a nonlocal phase field prior energy. We then combine the prior model with a data energy similar in spirit to that of Peng et al. [10] but at a single scale. We test the model on a VHR image of Beijing, and compare our results to other methods in the literature.

The rest of this paper is organised as follows. In section 2, we recall the essentials of phase field methods, and then describe our model. In section 3, we discuss the algorithms used to solve the model. In section 4, we describe experimental results on VHR images. We conclude in section 5.

2 The model: prior and data energies

As outlined in section 1, our aim is to find the region R in the image domain Ω that corresponds to the main roads in the road network contained in the image. We assume that we are given a region R_0 representing the road network at an (earlier) date than the image data. Our knowledge of R is then described by a probability distribution $P(R|I,R_0,K)$, where I is the image data, and K represents all other prior knowledge we may have. From this probability distribution, we can make estimates; in particular, we can compute a MAP estimate by finding the region with maximum probability, or alternatively with minimum negative log probability, or 'energy'. Rewriting $P(R|I,R_0,K)$ using Bayes' theorem, and making a reasonable independence assumption, we can express the energy to be minimized, up to an additive constant, as

$$E(R;I,R_0) = DE_P(R,R_0) + E_D(I,R)\,, \tag{1}$$

where E_P is the prior energy (D simply weights this term), and E_D is the data energy, and K is understood.

To compute anything, one must choose a mathematical representation for R. In this paper, we use a *phase field* representation, much used in physics and first introduced to image processing in [12]. A phase field $\phi : \Omega \to \mathbb{R}$ defines a region via a threshold z: $R = \{x : \phi(x) > z\}$. Furthermore, as we will see, the phase field prior energy is so constructed that the energy-minimizing phase field ϕ_R for a fixed region satisfies $\phi_R(x) \simeq 1$ for $x \in R$ and $\phi_R(x) \simeq -1$ for $x \in \bar{R}$, where $\bar{R} = \Omega \setminus R$. As a result, the quantities $\phi_\pm = (1 \pm \phi)/2$ are approximately equal to the characteristic functions of R and $\bar{R}$. The lack of any hard constraints on ϕ, *e.g.* that it should be a distance function, is responsible for the advantages of the phase field framework over other region modelling approaches [12].

With the representation decided, we can now describe the various terms in the energy as functionals of the phase field. We will abuse notation by using the same symbol for the energy as a function of ϕ and as a function of R.

2.1 Prior energy

The prior energy E_P is itself the sum of three pieces. The first, E_{P0}, is the basic phase field model, equivalent to a standard active contour with energy $\lambda_C L(\partial R) + \alpha_C A(R)$, where L is boundary length, A is region area, and λ_C and α_C are constants. This term ensures stability

of the model, boundary smoothness, and the characteristic function property mentioned earlier. The second, $E_{P,NL}$, is a nonlocal term coupling the phase field values at long distances. As shown in [12], it is equivalent to a quadratic higher-order active contour energy [13]. It introduces prior knowledge about the shapes of the regions occupied by all road networks; roughly speaking, that they are composed of long, low-curvature 'arms' of roughly constant width that join together at junctions. The third, $E_{P,GIS}$, introduces the prior knowledge specific to the road network of interest. It expresses the knowledge that R should be 'close' to R_0, which can also be described by its minimum energy phase field function ϕ_{R_0}. We now describe these pieces in more detail.

2.1.1 $E_{P,0}$ and $E_{P,NL}$

The basic phase field energy $E_{P,0}$ is given by the Ginzburg-Landau energy plus an odd parity term:

$$E_{P,0}(\phi) = \int_\Omega dx \left\{ \frac{1}{2}\nabla\phi(x)\cdot\nabla\phi(x) + W(\phi(x)) \right\}, \tag{2}$$

where the potential

$$W(y) = \lambda(\frac{1}{4}y^4 - \frac{1}{2}y^2) + \alpha(y - \frac{1}{3}y^3),$$

and λ and α are constants. For $\lambda \geqslant \alpha > 0$, W has two minima, at $y = -1$ and $y = 1$, and a maximum at $y = \alpha/\lambda$. If we ignore the gradient term, then for a fixed region R, with $z = \alpha/\lambda$, the energy-minimizing function, ϕ_R, takes value 1 inside and -1 outside R. The effect of the gradient term is to smooth this result, producing a narrow interface, centred around ∂R, that interpolates between 1 and -1.

The higher-order active contour phase field energy $E_{P,NL}$ introduces a long-range interaction between the values of ϕ at pairs of points separated by many pixels. It is given by

$$E_{P,NL}(\phi) = -\frac{\beta}{2}\iint_{\Omega^2} dx\,dx'\,\nabla\phi(x)\cdot\nabla\phi(x')\Psi((x-x')/d), \tag{3}$$

where d controls the range of the interaction. The interaction function, Ψ, is given by

$$\Psi(x) = \begin{cases} \frac{1}{2}\left(2 - |x| + \frac{1}{\pi}\sin(\pi|x|)\right) & \text{if } |x| < 2, \\ 0 & \text{else}. \end{cases}$$

In terms of ∂R, this interaction has two main effects: nearby boundary points tend to have parallel normal vectors, while those boundary points with antiparallel normal vectors increasingly repel one another as they approach closer than $2d$. These effects are responsible for the fact that the energy $E_{P,0} + E_{P,NL}$ favours regions composed of long, low curvature 'arms' of roughly constant width that join at junctions, or in other words, that it models network structures.

2.1.2 $E_{P,GIS}$

The final prior energy term, $E_{P,GIS}$, incorporates knowledge of the earlier road network, R_0. It takes the form

$$E_{P,GIS}(\phi, \phi_{R_0}) = \int_\Omega dx \left[\omega\phi_{R_0+}(x) + \bar{\omega}\phi_{R_0-}(x)\right]\left[\phi(x) - \phi_{R_0}(x)\right]^2. \tag{4}$$

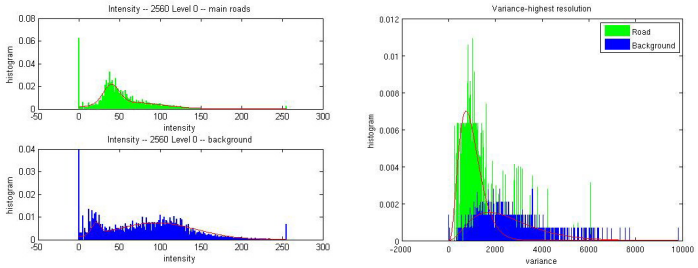

Figure 1: Histograms of the pixel intensities I on-road (top left) and off-road (bottom left), and of the variances V on-road (right, green/light grey) and off-road (right, blue/dark grey), and of the models fitted to them (solid lines).

The two terms correspond to the two components of the symmetric area difference between R and R_0: $x \in R \cap \bar{R}_0$ and $x \in \bar{R} \cap R_0$. These are separated so that they can be weighted differently by the parameters ω and $\bar{\omega}$. Because this term takes into account the exterior of R_0, it counteracts the background 'noise' appearing in the data.

2.2 Data energy

The data energy is the negative logarithm of $P(I|R,K)$. We assume that this factorizes as $P(I_R|R,K)P(I_{\bar{R}}|R,K)$, where subscripts indicate 'restricted to'. We use the same parameterized model for I_R and $I_{\bar{R}}$, the choice of model being based on a study of the image statistics. We model both the one point statistics of the image intensity, *i.e.* the histogram, and the two-point statistics, which we characterize by the variance $V(x)$ of the image in a small window around each pixel. Because of the factorization, the data energy is the sum of two pieces, one referring to R and one to $\bar{R}$ (indicated by overbars):

$$E_D(I,R) = -\int_\Omega dx \Big\{ \big[\ln P(I(x)) + \theta \ln Q(V(x))\big]\phi_+(x) + \big[\ln \bar{P}(I(x)) + \theta \ln \bar{Q}(V(x))\big]\phi_-(x) \Big\}. \quad (5)$$

Here P and $\bar{P}$ are two-component Gaussian mixture models, modelling the image intensities, while Q and $\bar{Q}$ are Gamma distributions, modelling the variances.

3 Implementation

3.1 Parameter estimation

The parameters of the Gaussian mixture and Gamma distributions are learned from the image data, using the known region R_0 to create samples of road and non-road. Note that the samples may contain errors, since R_0 does not correspond exactly to the road network in the image (see figure 2). The Gaussian mixture parameters are estimated using the EM algorithm, while the Gamma distribution parameters are estimated by least squares error minimization over the variance histograms computed in non-overlapping windows. Examples of histograms and the models fitted to them are shown in figure 1.

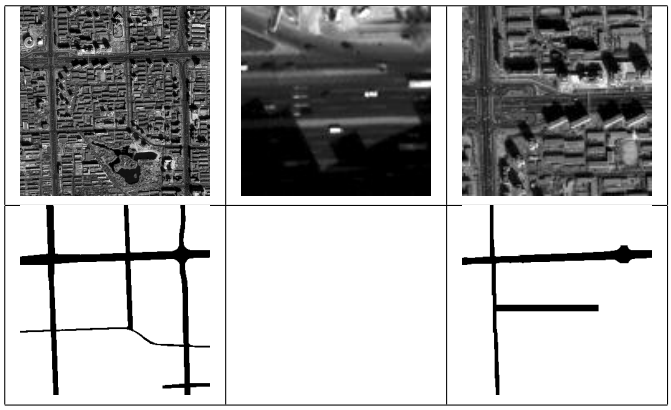

Figure 2: Top row, left to right: the QuickBird image used; a zoom on the image; a zoom on the reduced resolution image. Bottom row, left to right: ground truth, including smaller roads for comparison with other methods; deliberately 'damaged' ground truth, to simulate an earlier GIS map.

3.2 Energy minimization

The total energy functional, $E = E_D + D(E_{P,0} + E_{P,NL} + E_{P,GIS})$, is minimized with respect to ϕ using gradient descent. The functional derivative is

$$\frac{\delta E}{\delta \phi} = D\Big\{-\nabla^2\phi + \lambda(\phi^3 - \phi) + \alpha(1-\phi^2) + \beta\nabla^2\Psi * \phi + 2(\phi - \phi_{R_0})\big[\omega\phi_{R_{0+}} + \bar{\omega}\phi_{R_{0-}}\big]\Big\} - \frac{1}{2}\Big\{\big[\ln P(I(x)) + \theta \ln Q(V(x))\big] - \big[\ln \bar{P}(I(x)) + \theta \ln \bar{Q}(V(x))\big]\Big\}, \quad (6)$$

where $*$ indicates convolution. The neutral initialization was used.

4 Experimental results

The input data I was a QuickBird panchromatic image at 0.6m resolution, as shown in figure 2, which also shows a zoom on this image. An available GIS map from a few years earlier of the road network in the zone shown in the image was used in two ways: first, to create ground truth, for which it was slightly corrected via hand segmentation; and to create an inaccurate road network region to serve as R_0. Both these are also shown in figure 2. Note that R_0 has some roads added and some roads missing. Note also that smaller roads have been kept in the ground truth; this is to allow comparison with other methods, which attempt to find all roads, not just the main road network.

We tested and evaluated the model using the original QuickBird image (0.6m/pixel), and using a lower resolution version corresponding to the scaling coefficients of a Haar wavelet decomposition of the image at level 3, *i.e.* 4.8m resolution, where level 0 is full resolution. A zoom on this image is shown in figure 2. One can see that the image at level 3 has been simplified, but is still rather complex.

The rest of this section presents the results obtained at these two resolutions, with and without GIS information, *i.e.* with and without $E_{P,GIS}$. The results are compared to those obtained using three other methods: those of Bailloeul [2], an approach based on active

Level	D	α	λ	β	d	ω	$\bar{\omega}$	θ
3	200	0.0905	3	0.02	10	0	0	0.02
0	300	0.0905	3	0.02	80	0.00033 or 0	0.0006 or 0	0.02

Table 1: Parameter values used in the experiments. Note that apart from a change in the overall weight of the prior term, and the scaling of d due to the change of resolution, they are the same for the two resolutions.

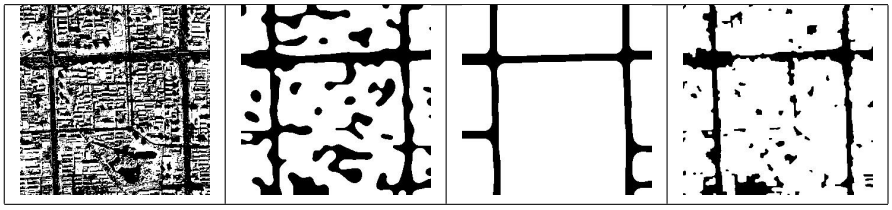

Figure 3: Experiment at reduced resolution, level 3 (320×320, road width $\simeq 12$ pixels). Three leftmost images: the thresholded phase field function at iterations 1 and 400, and at convergence, using the model without GIS information, *i.e.* without $E_{P,GIS}$. Rightmost image: for comparison, the result obtained when the nonlocal term $E_{P,NL}$ is dropped as well, leaving a model equivalent to a standard active contour. The importance of the prior geometric information carried by $E_{P,NL}$ is clear.

contours; Wang and Zhang [15], which uses classification, tracking, and morphology; Yu et al. [16], which creates a rough segmentation based on straight line density.

The parameter values for the prior energy were chosen by hand, but not freely. They are subject to a constraint that guarantees the Turing stability of the model, and a further constraint that ensures that a long bar of the desired road width is a stable configuration of the energy. The values used are given in table 1. Apart from a change in the overall weight of the prior term, and the scaling of d due to the change of resolution, they are the same for the two resolutions.

4.1 Results at reduced resolution

The leftmost three images in figure 3 show the thresholded phase field function at iterations 1 and 400 of gradient descent, and at convergence, using the model without GIS information, *i.e.* without $E_{P,GIS}$, but with the higher-order active contour prior knowledge, $E_{P,NL}$. The segmentation is very successful: the main road networks are retrieved nearly completely. The rightmost image shows the result obtained if $E_{P,NL}$ is omitted as well, leaving a model equivalent to a standard (*i.e.* not higher-order) active contour. The importance of the prior knowledge carried by the nonlocal term is clear.

By comparison, figure 4 shows the results obtained using the three methods mentioned above. The 'flexible active contour' method of Bailloeul (initially dedicated to building extraction) fails because it is not able to eliminate road sections that exist in the map but not in the image. On the other hand, the methods of Yu and Wang are able to detect the main road network and smaller roads, but, for both, the accuracy obtained in the delineation of the road boundary is poor, and the results show a great deal of noise. Some quantitative measures of the quality [6] of the results are shown in table 2.

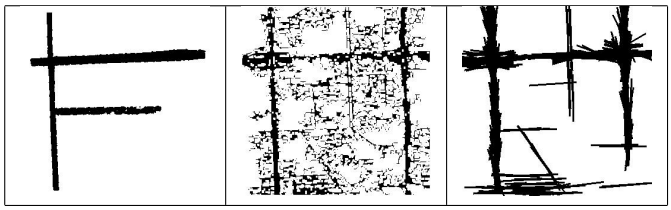

Figure 4: From left to right: the results obtained using the work of Bailloeul [2], Wang and Zhang [15], and Yu et al. [16], at reduced resolution.

Measure	Bailloeul	Wang	Yu	Our approach
TP/(TP+FN)	0.5003	0.6542	0.8240	0.7424
TP/(TP+FP)	0.7112	0.3784	0.4825	0.7382
TP/(TP+FP+FN)	0.4158	0.3153	0.4374	0.5876

Table 2: Quality measures of the different methods tested at reduced resolution (T = true, F = false, P = positive, N = negative).

4.2 Results at full resolution

The results obtained with our model, with and without GIS information, are illustrated in the leftmost two images in figure 5. The complexity of the image means that even with the prior knowledge carried by $E_{P,NL}$, without $E_{P,GIS}$ the model simply fails to retrieve the roads correctly. The addition of $E_{P,GIS}$ greatly improves the result. Its main effect is to eliminate false positives in the background, while preserving the correct segmentation of the roads themselves. To obtain this result, ω must be small, since the mistakes that may exist in the old map, should not affect the process, while $\bar{\omega}$ is somewhat bigger, because a strong constraint is needed to overcome the 'noise' in the background.

The right most image in figure 5 shows the result we obtain when we use as R_0, not the GIS map, but the result obtained at reduced resolution, level 3 (which did not use the GIS map either). This shows that in principle we can free ourselves from the need to have a GIS map available, and the full exploitation of this will be the subject of future work.

Figure 6 shows the results obtained with the methods of Bailloeul, Yu, and Wang at full resolution, while table 3 shows the corresponding quality measures.

5 Conclusion

We have proposed a model for the updating of road maps in dense urban areas by extracting the main road network from a VHR satellite image. Methodologically, our model is innovative in that it incorporates three different types of prior geometric knowledge: generic knowledge about smoothness; knowledge of the geometry of road networks in general; and knowledge of the specific road network at a different date, supplied as GIS data. Our results indicate that to work at full resolution, all three types of prior knowledge are essential, due to the great complexity of VHR images. However, one can free oneself from the need for GIS data by using instead a result obtained at lower resolution, where such knowledge appears not to be necessary provided the other two types are present. Our model gives better results than three other methods in the literature, even when smaller roads, which our model is not designed to detect, are included in the ground truth.

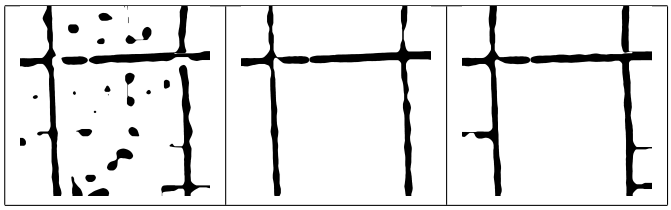

Figure 5: Experiments at full resolution, level 0 (2560×2560, road width $\simeq 96$ pixels). From left to right: the result obtained without GIS information, *i.e.* without $E_{P,GIS}$; the result obtained with GIS information, *i.e.* with $E_{P,GIS}$; the result obtained using the result obtained without $E_{P,GIS}$ at level 3 (figure 3) as a replacement for the GIS information.

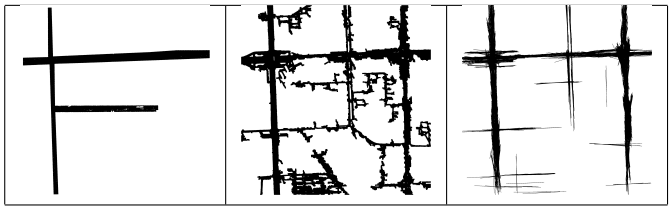

Figure 6: From left to right: the results obtained using the work of Bailloeul [2], Wang and Zhang [15], and Yu et al. [16], at full resolution.

Acknowledgments

This work was partially supported by European Union Network of Excellence MUSCLE (FP6-507752). The work of the first author is supported by an MAE/Alcatel/LIAMA grant. The authors would like to thank the Beijing Institute of Surveying and Mapping for providing the GIS data.

References

[1] P. Agouris, A. Stefanidis, and S. Gyftakis. Differential snakes for change detection in road segments. *Photogrammetric Engineering and Remote Sensing*, 67(12):1391–1399, February 2001.

[2] T. Bailloeul. *Active contours and prior knowledge for change analysis: Application to digital urban building map updating from optical high resolution remote sensing images*. PhD thesis, CASIA and INPT, October 2005.

[3] Y. Chen, H. Tagare, S. Thiruvenkadam, F. Huang, D. Wilson, K. Gopinath, R. Briggs, and E. Geiser. Using prior shapes in geometric active contours in a variational framework. *International Journal of Computer Vision*, 50(3):315–328, 2002.

[4] D. Cremers, F. Tischhäuser, J. Weickert, and C. Schnörr. Diffusion snakes: Introducing statistical shape knowledge into the mumford-shah functional. *International Journal of Computer Vision*, 50(3):295–313, 2002.

[5] M. F. A. Fortier, D. Ziou, C. Armenakis, and S. Wang. Automated correction and updating of road databases from high-resolution imagery. *Canadian Journal of Remote Sensing*, 27(1): 76–89, 2001.

Measure	Bailloeul	Wang	Yu	Our approach with GIS prior	Our approach with level 3 prior
TP/(TP+FN)	0.4769	0.8785	0.6706	0.6665	0.7130
TP/(TP+FP)	0.7612	0.4531	0.7836	0.9278	0.8290
TP/(TP+FP+FN)	0.4148	0.4264	0.5658	0.6336	0.6216

Table 3: Quality measures of the different methods tested at full resolution (T = true, F = false, P = positive, N = negative).

[6] C. Heipke, H. Mayr, C. Wiedemann, and O. Jamet. Evaluation of automatic road extraction. In *Proc. International Society for Photogrammetry and Remote Sensing (ISPRS)*, volume 32, 1997.

[7] M. Kass, A. Witkin, and D. Terzopoulos. Snakes: Active contour models. *International Journal of Computer Vision*, 1(4):321–331, 1988.

[8] M. E. Leventon, W. E. L. Grimson, and O. Faugeras. Statistical shape influence in geodesic active contours. In *Proc. IEEE Computer Vision and Pattern Recognition (CVPR)*, volume 1, pages 316–322, Hilton Head Island, South Carolina, USA, 2000.

[9] N. Paragios and M. Rousson. Shape priors for level set representations. In *Proc. European Conference on Computer Vision (ECCV)*, volume 2, pages 78–92, Copenhague, Danemark, 2002.

[10] T. Peng, I. H. Jermyn, V. Prinet, J. Zerubia, and B. Hu. Urban road extraction from vhr images using a multiscale approach and a phase field model of network geometry. In *Proc. 4th IEEE GRSS/ISPRS Joint Workshop on Remote Sensing and Data Fusion over Urban Areas (URBAN)*, Paris, France, April 2007.

[11] R. Péteri and T. Ranchin. Detection and extraction of road networks from high resolution satellite images. In *Proc. IEEE International Conference on Image Processing (ICIP)*, Barcelona, Spain, September 2003.

[12] M. Rochery, I. H. Jermyn, and J. Zerubia. Phase field models and higher-order active contours. In *Proc. IEEE International Conference on Computer Vision (ICCV)*, Beijing, China, October 2005.

[13] M. Rochery, I. H. Jermyn, and J. Zerubia. Higher-order active contours. *International Journal of Computer Vision*, 69(1):27–42, 2006.

[14] A. Srivastava, S. Joshi, W. Mio, and X. Liu. Statistical shape analysis: Clustering, learning, and testing. *IEEE Trans. Pattern Analysis and Machine Intelligence*, 27(4):590–602, April 2003.

[15] R. Wang and Y. Zhang. Extraction of urban road network using quickbird pan-sharpened multispectral and panchromatic imagery by performing edge-aided post-classification. In *Proc. International Society for Photogrammetry and Remote Sensing (ISPRS)*, Quebec City, Canada, October 2003.

[16] Z. Yu, V. Prinet, C. Pan, and P. Chen. A novel two-steps strategy for automatic gis-image registration. In *Proc. IEEE International Conference on Image Processing (ICIP)*, Singapore, 2004.